

**Robust and predictive 3D-QSAR models for predicting the activities of novel oxadiazole derivatives as multifunctional anti-Alzheimer agents**

**Yekai Sun<sup>a#</sup>, Zirou Zhang<sup>a#</sup>, Menghao Wen<sup>a</sup>, Fangfang Wang<sup>a\*</sup>, Xiuling Li<sup>a\*</sup>, Wei Yang<sup>b,c,d\*</sup> Bo Zhou<sup>e</sup>**

<sup>a</sup> School of Life Science, Linyi University, Linyi, 276000, China;

<sup>b</sup> National Clinical Research Center for Infectious Diseases, Shenzhen Third People's Hospital, 518112, Shenzhen, China;

<sup>c</sup> Shenzhen Clinical Research Center for Tuberculosis, Shenzhen, People's Republic of China;

<sup>d</sup> Warshel Institute for Computational Biology, School of Science and Engineering, The Chinese University of Hong Kong, 518172, Shenzhen, China;

<sup>e</sup> State Key Laboratory of Functions and Applications of Medicinal Plants, College of Basic Medical, Guizhou Medical University, Guizhou, 550004, China.

\* Corresponding author

E-mail: yu100288@163.com

# These authors contributed equally to this work.

Table S1. Summary of template ligand-based QSAR results.

	CoMFA	CoMSIA							
	SE	S	E	H	D	A	SE	SH	SD
R <sup>2</sup> <sub>cv</sub>	0.692	0.685	0.680	0.694	0.689	0.678	0.686	0.695	0.692
R <sup>2</sup> <sub>ncv</sub>	0.818	0.708	0.705	0.712	0.708	0.702	0.710	0.717	0.714
SEE	0.260	0.265	0.267	0.263	0.265	0.268	0.264	0.261	0.263
F	21.670	20.570	20.290	20.996	20.639	20.050	20.762	21.519	21.179
R <sup>2</sup> <sub>pred</sub>	0.6885	0.6933	0.6072	0.6732	0.6034	0.6129	0.6829	0.6567	0.6835
SEP	0.313	0.316	0.318	0.313	0.315	0.319	0.316	0.312	0.313
N <sub>C</sub>	2	2	2	2	2	2	2	2	2
<b>Field contribution</b>									
S	0.078	0.033	-	-	-	-	0.032	0.031	0.032
E	0.006	-	0.017	-	-	-	0.017	-	-
H	-	-	-	0.046	-	-	-	0.044	-
D	-	-	-	-	0.022	-	-	-	0.021
A	-	-	-	-	-	0.019	-	-	-
RDF060p	0.303	0.333	0.345	0.325	0.338	0.346	0.324	0.304	0.316
Mor20e	0.277	0.296	0.303	0.289	0.297	0.304	0.291	0.279	0.286
Mor28m	0.336	0.338	0.334	0.340	0.342	0.331	0.336	0.342	0.344
<b>CoMSIA</b>									
	SA	EH	ED	EA	HD	HA	DA	SEH	SED

R <sup>2</sup> <sub>cv</sub>	0.686	0.694	0.690	0.681	0.699	0.625	0.690	0.692	0.691
R <sup>2</sup> <sub>ncv</sub>	0.708	0.714	0.710	0.705	0.718	0.967	0.708	0.719	0.715
SEE	0.265	0.263	0.264	0.267	0.261	0.107	0.265	0.260	0.262
F	20.574	21.192	20.853	20.268	21.659	49.597	20.656	21.700	21.371
R <sup>2</sup> <sub>pred</sub>	0.6889	0.6649	0.6937	0.6012	0.6655	0.4361	0.6988	0.6490	0.6742
SEP	0.316	0.313	0.314	0.318	0.311	0.357	0.314	0.313	0.314
N <sub>C</sub>	2	2	2	2	2	7	2	2	2
<b>Field contribution</b>									
S	0.033	-	-	-	-	-	-	0.031	0.032
E	-	0.017	0.017	0.017	-	-	-	0.016	0.016
H	-	0.045	-	-	0.045	0.545	-	0.043	-
D	-	-	0.022	-	0.021	-	0.022	-	0.021
A	0.018	-	-	0.019	-	0.068	0.019	-	-
RDF060p	0.324	0.315	0.328	0.336	0.308	0.125	0.329	0.295	0.307
Mor20e	0.291	0.285	0.293	0.298	0.281	0.127	0.293	0.276	0.283
Mor28m	0.334	0.338	0.340	0.330	0.345	0.135	0.338	0.340	0.341
<b>CoMSIA</b>									
	SEA	SHD	SHA	SDA	EHD	EHA	EDA	HDA	SEHD
R <sup>2</sup> <sub>cv</sub>	0.686	0.694	0.693	0.691	0.696	0.694	0.690	0.616	0.690
R <sup>2</sup> <sub>ncv</sub>	0.710	0.723	0.718	0.714	0.820	0.714	0.711	0.966	0.725
SEE	0.264	0.258	0.261	0.262	0.260	0.262	0.264	0.108	0.257
F	20.777	22.228	21.600	21.239	21.852	21.229	20.877	48.597	22.403
R <sup>2</sup> <sub>pred</sub>	0.6791	0.6523	0.6545	0.6799	0.6887	0.6612	0.6891	0.4005	0.6460
SEP	0.316	0.313	0.313	0.314	0.312	0.313	0.314	0.362	0.314
N <sub>C</sub>	2	2	2	2	2	2	2	7	2
<b>Field contribution</b>									
S	0.032	0.031	0.031	0.032	-	-	-	-	0.030
E	0.016	-	-	-	0.016	0.016	0.017	-	0.015
H	-	0.042	0.043	-	0.044	0.044	-	0.492	0.041
D	-	0.020	-	0.021	0.020	-	0.021	0.083	0.019
A	0.018	-	0.017	0.018	-	0.018	0.018	0.084	-
RDF060p	0.315	0.289	0.295	0.307	0.299	0.306	0.319	0.101	0.280
Mor20e	0.287	0.273	0.276	0.283	0.278	0.281	0.288	0.131	0.271
Mor28m	0.332	0.345	0.338	0.339	0.343	0.334	0.336	0.110	0.343
<b>CoMSIA</b>									
	SEHA	SEDA	SHDA	EHDA	SEHDA				
R <sup>2</sup> <sub>cv</sub>	0.690	0.689	0.692	0.695	0.688				
R <sup>2</sup> <sub>ncv</sub>	0.719	0.716	0.725	0.721	0.726				
SEE	0.260	0.261	0.258	0.259	0.257				
F	21.794	21.442	22.367	21.949	22.553				
R <sup>2</sup> <sub>pred</sub>	0.6475	0.6724	0.6526	0.6571	0.6470				
SEP	0.314	0.314	0.313	0.312	0.315				
N <sub>C</sub>	2	2	2	2	2				

Field contribution					
S	0.030	0.031	0.030	-	0.029
E	0.016	0.016	-	0.016	0.015
H	0.042	-	0.042	0.043	0.041
D	-	0.020	0.020	0.020	0.019
A	0.017	0.017	0.017	0.017	0.017
RDF060p	0.286	0.298	0.280	0.291	0.273
Mor20e	0.237	0.279	0.270	0.275	0.269
Mor28m	0.336	0.337	0.341	0.338	0.338

Table S2. Summary of receptor-based QSAR results.

	CoMFA	CoMSIA							
	SE	S	E	H	D	A	SE	SH	SD
$R^2_{cv}$	0.604	0.604	0.599	0.590	0.593	0.586	0.597	0.592	0.593
$R^2_{ncv}$	0.776	0.735	0.757	0.732	0.759	0.741	0.789	0.766	0.792
SEE	0.232	0.252	0.242	0.254	0.241	0.250	0.226	0.237	0.224
F	29.421	23.617	26.423	23.202	26.772	24.294	31.725	27.815	32.285
$R^2_{pred}$	0.6293	0.6109	0.6652	0.6100	0.5996	0.6424	0.6773	0.6127	0.6069
SEP	0.309	0.309	0.311	0.314	0.313	0.316	0.312	0.313	0.313
$N_C$	2	2	2	2	2	2	2	2	2
Field contribution									
S	0.090	0.078	-	-	-	-	0.076	0.079	0.078
E	0.132	-	0.163	-	-	-	0.157	-	-
H	-	-	-	0.096	-	-	-	0.096	-
D	-	-	-	-	0.157	-	-	-	0.150
A	-	-	-	-	-	0.115	-	-	-
RDF060p	0.251	0.317	0.267	0.306	0.279	0.295	0.238	0.271	0.251
Mor20e	0.230	0.270	0.254	0.272	0.243	0.265	0.231	0.243	0.221
Mor28m	0.297	0.336	0.317	0.326	0.321	0.325	0.298	0.312	0.300
CoMSIA									
	SA	EH	ED	EA	HD	HA	DA	SEH	SED
$R^2_{cv}$	0.588	0.576	0.579	0.573	0.574	0.569	0.569	0.571	0.575
$R^2_{ncv}$	0.774	0.787	0.812	0.794	0.792	0.773	0.797	0.815	0.835
SEE	0.233	0.226	0.213	0.223	0.224	0.234	0.221	0.211	0.199
F	29.133	31.452	36.613	32.792	32.307	28.973	33.271	37.457	43.057
$R^2_{pred}$	0.6520	0.6817	0.6818	0.7253	0.6052	0.6552	0.6524	0.6944	0.6936
SEP	0.315	0.319	0.318	0.321	0.320	0.322	0.322	0.321	0.320
$N_C$	2	2	2	2	2	2	2	2	2
Field contribution									
S	0.077	-	-	-	-	-	-	0.073	0.069
E	-	0.159	0.152	0.151	-	-	-	0.148	0.140

H	-	0.092	-	-	0.095	0.094	-	0.086	-
D	-	-	0.144	-	0.153	-	0.146	-	0.133
A	0.113	-	-	0.110	-	0.116	0.112	-	-
RDF060p	0.263	0.224	0.210	0.221	0.237	0.249	0.233	0.205	0.196
Mor20e	0.239	0.236	0.219	0.235	0.224	0.242	0.224	0.221	0.208
Mor28m	0.308	0.288	0.275	0.283	0.291	0.298	0.285	0.268	0.255
<b>CoMSIA</b>									
	SEA	SHD	SHA	SDA	EHD	EHA	EDA	HDA	SEHD
R <sup>2</sup> <sub>cv</sub>	0.568	0.571	0.565	0.567	0.555	0.547	0.551	0.547	0.552
R <sup>2</sup> <sub>ncv</sub>	0.820	0.819	0.803	0.823	0.835	0.819	0.836	0.823	0.853
SEE	0.208	0.209	0.218	0.207	0.199	0.209	0.199	0.206	0.188
F	38.733	38.551	34.643	39.439	43.030	38.435	43.236	39.532	49.419
R <sup>2</sup> <sub>pred</sub>	0.7356	0.6165	0.6658	0.6621	0.6975	0.7419	0.7389	0.6640	0.7008
SEP	0.323	0.321	0.324	0.323	0.327	0.330	0.329	0.330	0.329
N <sub>C</sub>	2	2	2	2	2	2	2	2	2
<b>Field contribution</b>									
S	0.069	0.074	0.074	0.070	-	-	-	-	0.063
E	0.140	-	-	-	0.140	0.140	0.132	-	0.128
H	-	0.088	0.089	-	0.081	0.082	-	0.084	0.074
D	-	0.142	-	0.136	0.135	-	0.126	0.136	0.1239
A	0.103	-	0.110	0.104	-	0.104	0.097	0.105	-
RDF060p	0.204	0.218	0.226	0.215	0.186	0.194	0.188	0.204	0.178
Mor20e	0.221	0.209	0.224	0.210	0.214	0.227	0.216	0.216	0.206
Mor28m	0.263	0.269	0.277	0.265	0.245	0.253	0.241	0.254	0.228
<b>CoMSIA</b>									
	SEHA	SEDA	SHDA	EHDA	SEHDA				
R <sup>2</sup> <sub>cv</sub>	0.543	0.548	0.545	0.530	0.529				
R <sup>2</sup> <sub>ncv</sub>	0.840	0.853	0.844	0.851	0.864				
SEE	0.197	0.188	0.194	0.190	0.181				
F	44.479	49.381	45.841	48.474	54.208				
R <sup>2</sup> <sub>pred</sub>	0.7429	0.7348	0.6669	0.7350	0.7250				
SEP	0.332	0.330	0.331	0.336	0.337				
N <sub>C</sub>	2	2	2	2	2				
<b>Field contribution</b>									
S	0.064	0.060	0.065	-	0.055				
E	0.129	0.121	-	0.119	0.110				
H	0.075	-	0.077	0.069	0.064				
D	-	0.116	0.125	0.116	0.107				
A	0.096	0.089	0.096	0.089	0.082				
RDF060p	0.184	0.180	0.193	0.175	0.170				
Mor20e	0.217	0.208	0.206	0.214	0.208				
Mor28m	0.236	0.226	0.236	0.217	0.204				

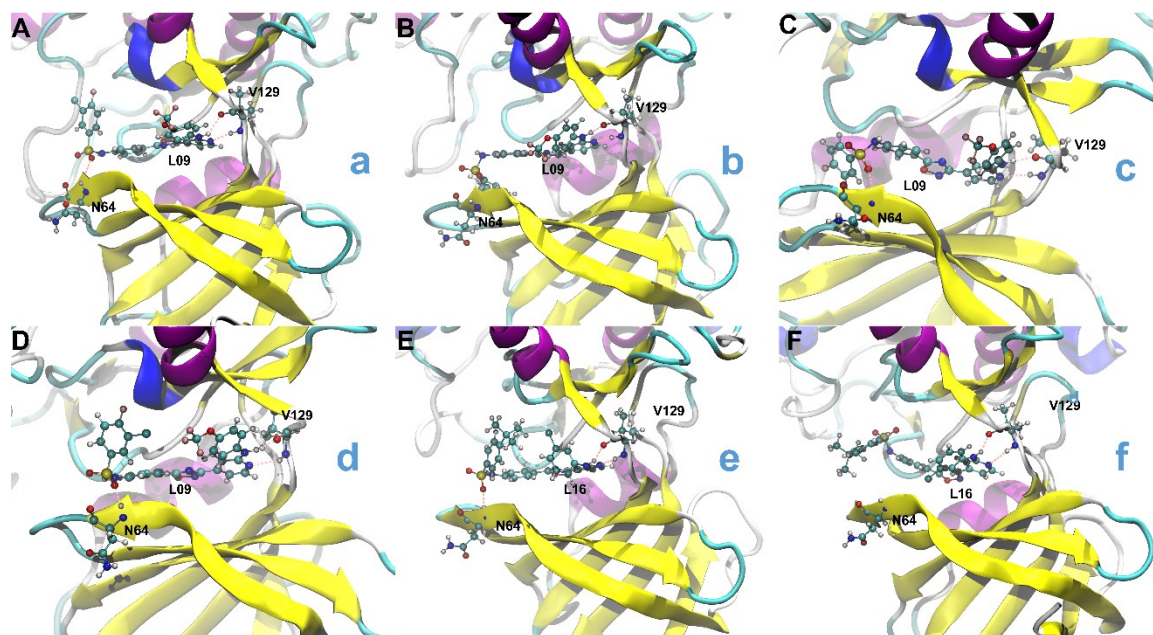


**Fig. S1 Representative structures of metastable states.** The representative structures of each metastable state during the MD simulations are shown. Panels A-F correspond to states a to f. The protein is depicted using the New Cartoon representation, while L09, L16, and key residues are shown using balls and sticks.

**Table S3. Binding Affinity Calculations for L09 and L16.** The binding affinities for L09 and L16 with the receptor GSK3 $\beta$  were calculated using the GBSA and PBSA methods, respectively.

Energy terms	L09		L16	
GBSA				
Energy Component	Average	Std. Err. of Mean	Average	Std. Err. of Mean
VDWAALS	-53.2787	0.0713	-51.5581	0.05
EEL	-25.3926	0.0653	-21.7004	0.0898
EGB	46.4078	0.0594	41.5526	0.0843
ESURF	-6.9815	0.0083	-6.5051	0.0056
DELTA G gas	-78.6713	0.0949	-73.2585	0.1025
DELTA G solv	39.4263	0.0558	35.0476	0.0819
DELTA TOTAL	-39.2449	0.0626	-38.2109	0.0503
DELTA S total	-26.5418	0.4784	-24.7703	0.641
Binding (GBSA)	-12.7031	0.541	-13.4406	0.6913
PBSA				
Energy Component	Average	Std. Err. of Mean	Average	Std. Err. of Mean
VDWAALS	-53.2787	0.0713	-51.5581	0.05

EEL	-25.3926	0.0653	-21.7004	0.0898
EPB	50.3688	0.0741	46.5303	0.1001
ENPOLAR	-5.2896	0.0044	-5.1255	0.0032
EDISPER	0	0	0	0
DELTA G gas	-78.6713	0.0949	-73.2585	0.1025
DELTA G solv	45.0792	0.0716	41.4048	0.0987
DELTA TOTAL	-33.5921	0.0554	-31.8537	0.0553
DELTA S total	-26.5418	0.4784	-24.7703	0.641
Binding (PBSA)	-7.0503	0.5338	-7.0834	0.6963

**Table S4. H-bond occupancy during simulations.** The H-bond occupancy rates were calculated based on the sum of replicates in the two MD systems, respectively.

GSK3 $\beta$ -L09			GSK3 $\beta$ -L16		
donor	acceptor	occupancy	donor	acceptor	occupancy
L09	Val129	41.80%	L16	Val129	20.73%
Lys177	L09	0.16%	L16	Asp194	5.87%
Val129	L09	3.88%	Lys177	L16	0.78%
L09	Asp194	0.24%	Val129	L16	4.31%
Asn180	L09	0.36%	Asn180	L16	10.23%
Gln179	L09	0.31%	L16	Asn180	0.15%
Asn64	L09	6.48%	Gln179	L16	0.07%
L09	Asn64	0.45%	Arg214	L16	0.04%
Gly65	L09	0.01%	Lys85	L16	0.12%
Gln179	L09	0.01%	L16	Gln179	0.69%
Arg135	L09	0.04%	Ser66	L16	0.11%
Asn64	L09	0.01%	Asn64	L16	3.25%
Ser66	L09	0.03%	L16	Asn64	0.69%
Arg135	L09	0.01%	Tyr128	L16	0.01%
Lys60	L09	0.01%	L16	Ser66	0.07%
Tyr128	L09	0.01%	Ser66	L16	0.01%